Simulation of Elastic and Plastic Response in the Glassy Polycarbonate of 4,4′-Isopropylidenediphenol

M. Hutnik† and A. S. Argon*,‡

Departments of Materials Science and Engineering and Mechanical Engineering, Massachusetts Institute of Technology, Cambridge, Massachusetts 02139

U. W. Suter§

Institut für Polymere, ETH-Zürich, CH-8092 Zürich, Switzerland

Received July 21, 1992; Revised Manuscript Received November 30, 1992

ABSTRACT: The previously determined molecular structure model of the dense, glassy polycarbonate of 4,4′-isopropylidenediphenol ("Bisphenol A polycarbonate" (PC)) has been used in conjunction with the structure-probing techniques of Theodorou and Suter and those of Mott et al. developed for atactic polypropylene (PP) to determine the small-strain elastic constants and study the mechanisms of large-strain plastic deformation of PC. The calculated elastic moduli of the microstructures all fall above the experimentally reported range but are not considered unreasonable in view of the relatively small size of the simulation cell and the rigidity of the PC repeat unit. For large-strain deformation, the ensemble-average stress–strain response exhibits a linear region parallel to the elastic loading line up to about 6–7% shear strain, where yielding is found to occur. Large-strain plastic shearing consists of a series of reversible elastic loading steps followed by irreversible plastic rearrangements. This behavior and its molecular interpretation are closely similar to what was found by Mott et al. in PP. The response of the ensemble shows a decrease in initial hydrostatic pressure with increasing strain, indicating that the initial state of the material has a strong tendency to densify upon plastic deformation. It is shown that the plastic response of the material is at least partly responsible for the pressure decrease that occurs during the deformation. This shear-induced pressure response in PC is opposite to that found in PP, where an initial dilatant response was found. Analysis of the stress drops indicated that plastic response is a result of shear transformations with an average transformation shear strain of 1.2%. Contrasting this finding with experimentally determined shear activation volumes leads to the conclusion that the shear transformations in bulk PC must occur in clusters of diameter of about 10.1 nm, indicating that the cooperative movement of many chain segments are involved in a single plastic relaxation event. The molecular movements associated with plastic flow were investigated. The applied strain increments could be partitioned into large phenylene ring rotations, carbonate group reorientations, and isopropylidene group rearrangements during the plastic events. However, none of these specific movements were found individually dominant. They appeared rather as kinematically necessary contributions to the overall transformation strain in the ca. 10.1-nm clusters.

1.0. Introduction

Microstructures of the dense, glassy polycarbonate of 4,4′-isopropylidenediphenol (Bisphenol A polycarbonate (PC)) have been simulated and well characterized in three previous associated studies (referred to here as I, II, and III), displaying very good agreement with various experimental microscopic quantities.[1-3] These PC microstructures have been used to investigate the mechanical behavior of PC ranging from the small-strain elastic to the large-strain plastic response of the structure. In this study first the elastic properties of the microstructures are presented. This is followed by the results of a simulation of the large-strain plastic response.

The molecular-level origins of plastic deformation of amorphous glassy polymers and their influence on macroscopic behavior have been of longstanding interest. Direct experimental observation of plastic events on the atomistic scale in these systems is difficult to achieve. A number of theoretical models have been postulated about the local molecular-level motions that lead to plastic flow. These models concentrate on the premise that the localized motion of some idealized and distinct characteristic chain element is in large part responsible for the plastic deformation. Separate from the theoretical models, computer simulations have also been carried out to furnish a better understanding of the elastic and plastic behavior on the molecular level. In this direction there have been a number of simulations of the plastic behavior of metallic glasses in which the kinematics of the atomic rearrangements are relatively simple. In comparison to these, only a few studies have involved glassy polymers. One such recent study by Mott, Argon, and Suter[4] (hereafter referred to as MAS) based upon the original methodology developed by Theodorou and Suter[5,6] on atactic polypropylene (PP) has developed an entirely new approach to dealing with this complex problem. While the study of MAS has provided considerable insight into the plastic rearrangements in chain molecules, the very simplicity of the molecular microstructure of PP has revealed little structural detail in the plastic relaxations. Therefore, investigation of these phenomena in a polymer with more molecular-level structure such as PC was considered to be most desirable.

Specifically for PC, the molecular-level structure and the motions that are present in an unstressed state have

* To whom correspondence should be addressed.
† Department of Materials Science and Engineering. Current address: Department of Chemical Engineering, Massachusetts Institute of Technology, Cambridge, MA 02139.
‡ Department of Mechanical Engineering.
§ Formerly of the Department of Chemical Engineering, Massachusetts Institute of Technology, Cambridge, MA 02139.

0024-9297/93/2226-1097$04.00/0

been widely studied by several volume-averaging techniques. Nuclear magnetic resonance, dynamic mechanical spectroscopy, infrared dichroism, and wide-angle X-ray and neutron scattering are among the many experimental techniques that have been used to probe the structure and segmental dynamics of PC, concentrating on the localized chain arrangements and motions. These have been reviewed in detail by Hutnik et al. in II and III. For PC undergoing plastic deformation, the experimental research into the atomistic-level behavior has been quite limited. In response to this need we now report below the results of a simulation utilizing these microstructures to investigate the plastic deformation of PC, based upon the work of MAS on PP. Here we have concentrated our efforts in the study of the motion of specific molecular groups and on the similarities and differences between the behavior of PP and PC, particularly in reference to the more structured nature of the PC molecule.

2.0. Previous Work

One starting point to study the mechanical behavior of a system is to probe its elastic properties. Calculation of elastic constants has been done on a wide variety of atomistic, nonbonded systems. Numerous computational techniques, including molecular dynamics (MD) and Monte Carlo (MC) simulations on both cystalline[7-11] and amorphous systems,[12-15] have been performed.

The amount of research has been less extensive for bonded systems. Tashiro, Kobayashi, and Tadokoro calculated the elastic moduli of several crystalline polymers.[16,17] In the first detailed atomistic study of an amorphous glassy polymer, Theodorou and Suter[5] computed the small-strain elastic response of atactic polypropylene by two different approaches. The first was based on changes in the total potential energy of the structures with applied small-strain increments (the "energy" approach), and the second was based on the volume-average change in the atomic-level stress tensors (the "force" approach). The elastic constants predicted by these two approaches were closely similar and gave good agreement with experimental results.

In a more recent study, Clarke and Brown[18] used MD to simulate the uniaxial deformation in tension of an amorphous dense system of polyethylene-like chains. Their calculated Young's modulus and Poisson's ratio were in reasonable agreement with experimental results.

In the investigation of the small-strain elastic response of PC reported here, we have chosen to calculate the elastic constants with the "energy" approach mentioned above and described in detail by Theodorou and Suter[5] (see also Weiner[19]).

In the study of the inelastic response of polymeric solids, infrared spectroscopy and, more particularly, infrared dichroism have been used to obtain direct experimental observations of chain movement under the application of external stress.[20,21] Specifically, Jansson and Yannas,[20] who used infrared dichroism to study glassy PC at small strains, observed that the onset of chain rotation and viscoelastic response could be detected between 0.6 and 1% strain at room temperature. Lunn and Yannas[21] used the same technique to investigate the behavior of the same polymer at larger strains, up to 6%, and noted that in the homogeneous region of deformation the main-chain backbone changed orientation up to 2°.

Many ad hoc molecular segment level models have been constructed to provide a theoretical framework for the plastic deformation of glassy polymers. Among these that are relevant to our present study are those by Robertson,[22] Argon,[23] and Yannas.[24] Robertson's[22] theory is based upon the concept that molecules exist in two states, a low-energy trans state and a high energy cis state, also termed as a *flexed* state. When a stress is applied, intramolecular transitions between the two conformations increase the local energy to a state corresponding to that above the glass transition temperature (in the unstressed state) and therefore allowing for plastic flow to occur. The theory by Argon[23] considers thermally activated rotations of small molecular segments under an applied stress, from a random orientation to an orientation parallel to the principal extension direction. The movement of the segments is resisted by the surrounding molecules, which are collectively treated as an elastic continuum, resulting in a model for the temperature and strain rate dependence of the plastic shear resistance. The theory of Yannas[24] also considers the localized motion of small groups of molecular segments, termed "strophon", which refers to a segment of three virtual bonds. The uncoiling motion of these by backbone rotations is envisioned to produce local inelastic relaxation.

A less molecularly specific theory, borrowing from models of plasticity of glassy metals, is that of Oleynik,[25] who attributes plastic flow to local shear transformations, occurring under stress. The local regions that undergo a succession of such transformations eventually reached a relaxed final deformed state.

In a study of the energetics of strain-induced intramolecular conformational transitions of single chains, Bleha, Gajdos, and Karasz[26] suggest that such transitions could be a mechanism for inelastic behavior.

Simulations of plastic deformation have been performed by many investigators for nonbonded amorphous materials. Of these, some examples intended for metallic glasses are relevant to our study. Plastic shearing of atomic glasses has been simulated in two dimensions by Argon and Shi[27] using a Bragg bubble raft and by Deng, Argon, and Yip[14] by computer molecular dynamics. In both cases Argon and co-workers have concluded that plastic deformation occurs by local shear transformations, preferentially in clusters that had an excess of free volume. These were identified by Deng et al. more specifically as "liquid-like" material. These two-dimensional studies are oversimplified. They avoid many complexities that arise in three-dimensional simulations but still provide very insightful results.

Maeda and Takeuchi[12] and Srolovitz, Vitek, and Egami[13] studied the three-dimensional deformation behavior of nonbonded model materials with a molecular dynamics approach and have used the important concept of atomic-level stress tensors to study local atom environments where inelastic strains are produced. They found that plastic deformation by inhomogeneous atom movements occurred in well-defined, localized regions characterized by high atomic-level shear stresses, which can be much greater than the applied stress. While these studies on atomic glasses have been very informative, they lack the important internal constraints characteristic of the chain molecule of the polymeric glass.

Among the simulations of the atomistic-level response to deformation, that of Theodorou and Suter[5,6] is the most relevant to our approach. They have used their molecular structure models to explore deformations under stress, by making use of the notion of atomic-level stresses used by Srolovitz et al.,[13] in a modified form to include the effect of torques acting between some bonded atoms. They simulated the elastic deformation of PP and studied the changes of the atomic-level stresses upon deformation and

other microstructural changes, such as the change in the segment rotation angles. However, they did not specifically study the kinematics of localized inelastic deformation events.

Termonia and Smith[28-30] have developed a kinetic model for tensile deformation of solid amorphous polymers by representing the system as a network in which weak intermolecular bonds tie the chains together. During deformation these bonds are allowed to break by a Monte Carlo process based upon overcoming an activation barrier. Comparisons of the results with experiments on melt-crystallized polyethylene have given good qualitative agreement.

Clarke and Brown[18] in their aforementioned study also modeled uniaxial tensile deformation using constant-stress molecular dynamics (MD). The occurrence of yielding and plastic flow were reported. The usual time scale restrictions characteristic of the MD method, however, limit the extent to which the results can be compared with experiments.

The plastic deformation of PP based upon the work of Theodorou and Suter has been carried out by Mott, Argon, and Suter[4] (MAS). This is to date the most extensive simulation of the plastic deformation of a glassy polymer. It includes not only the atomic-level stress tensor but also introduces the concept of an atomic-level strain increment tensor! The major conclusion of this work is that plastic deformation of PP is dilatant in early stages and that it occurs in a jerky manner during large irreversible stress drops associated with complex and cooperative small conformational rearrangements. In these rearrangements no single recurring molecular mechanism could be identified as being responsible for the production of plastic strain. Through analysis of the simulation results and comparing these with experiments, MAS have shown that in a typical flexible-chain glassy polymer local plastic relaxations occur in quite large clusters on the order of 8–10 nm in size.

The techniques developed by MAS for plastic deformation have been used in the present study of plastic deformation of PC. In what follows we present the results of this study and make extensive comparisons of the two studies.

3.0. Modeling of the Small-Strain Elastic Deformation

Amorphous PC microstructures were generated by the modeling technique described in II.[2] These represent static models of dense, disordered packings of a density of 1.20 g/cm^3, appropriate to a temperature of 300 K, and of minimum (local) potential energy. The microstructures can be described as 0 K models at a density corresponding to the temperature of interest. Thermal effects are included in the structures only in an average fashion through the use of the correct density appropriate to room temperature. In this sense the model contains in an indirect way the *effects* of the vibrational entropies of atoms that have resulted in anharmonic modulus reductions due to thermal expansion. Spatial periodic continuation conditions are employed for the cubic simulation cell. The bond angles and bond lengths are fixed. Molecular rearrangement occurs only through changing the torsion angles of the bonds and the overall orientation of the chain. Coulombic interactions are included.

Thirteen independent microstructures have been generated with periodic cube edge lengths of 1.844 nm, representing a degree of polymerization of 35 (MW = 4532) and containing 485 atoms or atom groups in each cube. Two larger sized microstructures have also been completed, which had periodic cube edge lengths of 2.987 nm, with a degree of polymerization of 151 (MW =19 264) and containing 2051 atoms or atom groups in the cube.

The calculation of the elastic constants have employed the "energy" approach of Theodorou and Suter.[5] These authors have also used a "force" (atomic-level stress) approach to calculate the elastic constants. This approach, which is fundamentally equivalent to the energy approach, is more tedious to implement and provides no greater insight for the calculation of only elastic properties. It is, of course, the only meaningful method for the study of large-strain deformation. In the energy approach the tensor of isothermal elastic coefficients of an isotropic material are obtained through the operations

$$c_{LMNK} = \left(\frac{\partial \tau_{LM}}{\partial \epsilon_{NK}}\right)_T = \frac{1}{V_0}\left(\frac{\partial^2 A}{\partial \epsilon_{LM}\,\partial \epsilon_{NK}}\right)_T \tag{1}$$

where τ_{LM} are the elements of the global stress tensor, while ϵ_{LM} are the elements of the imposed infinitesimal strain tensor, V_0 is the volume of the undeformed state, and A is the Helmholtz free energy.[5,19] The well-known contracted Voigt notation for stresses and strains is used in which the elastic constants for an isotropic material are defined as

$$c_{11} = 2\mu + \lambda \tag{2a}$$

$$c_{12} = \lambda \tag{2b}$$

$$c_{44} = \mu \tag{2c}$$

where λ and μ are known as the Lamé constants. The Young's modulus, E, the shear modulus, G, the bulk modulus, B, and the Poisson's ratio, ν, can then be given in terms of λ and μ as

$$E = \mu\frac{3\lambda + 2\mu}{\lambda + \mu} \tag{3a}$$

$$G = \mu \tag{3b}$$

$$B = \lambda + \frac{2}{3}\mu \tag{3c}$$

$$\nu = \frac{\lambda}{2(\lambda + \mu)} \tag{3d}$$

Since entropy is not specifically considered, the Helmholtz free energy can be replaced by the total potential energy U^{pot} of the structure, and the elastic constants can then be obtained by generic operations such as

$$\left(\frac{\partial^2 A}{\partial \epsilon^2}\right)_T = \left(\frac{\partial^2 U^{pot}}{\partial \epsilon^2}\right)_T \tag{4}$$

where ϵ stands for the specific increment of the form of imposed strain.

Three types of deformation—uniform hydrostatic compression, pure shear, and pure uniaxial tension—were used to directly obtain the various isotropic elastic moduli from operations of the type given in eq 4. Thus, for hydrostatic compression to obtain the bulk modulus B we take ϵ as the negative of the dilatation, i.e., $(-\Delta V/V)$; for simple shear to obtain the shear modulus G we take ϵ as the shear strain γ; and finally to obtain c_{11} we take ϵ as a uniaxial tensile strain (keeping all other strain increments zero). Thus,

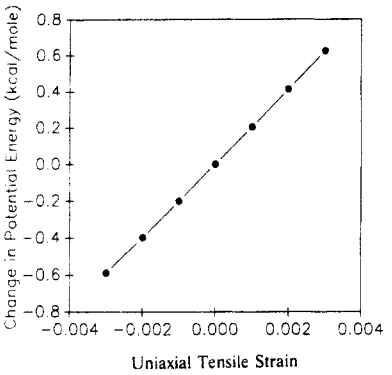

Figure 1. Example of the system potential energy, U^{pot}_{min}, plotted as a function of the uniaxial tensile strain for a uniaxial tensile simulation of a microstructure with a starting cube edge length of 1.8 nm.

more specifically, we obtain

$$B = \frac{1}{V_0}\left(\frac{\partial^2 U^{pot}_{min}}{\partial \epsilon^2}\right)_T \quad (5)$$

$$G = \frac{1}{V_0}\left(\frac{\partial^2 U^{pot}_{min}}{\partial \gamma^2}\right)_T \quad (6)$$

$$c_{11} = \frac{1}{V_0}\left(\frac{\partial^2 U^{pot}_{min}}{\partial \epsilon^2}\right)_T \quad (7)$$

These deformations were separately imposed upon the individual microstructures by modifying the continuation vectors of the system. This changes the position of the parent chain with respect to the positions of its neighbor images, thereby shifting the system away from its energy minimum. The system energy then can be reminimized to reach its deformed equilibrated state. Affine transformations cannot be imposed for obvious reasons.[5] The details of how such system strain increments are imposed by systematic border displacements on the simulation cell (extension or rotation of continuation vectors) have been described adequately elsewhere[5] and will not be repeated here. It suffices to state that the border displacements are chosen to be very small ($\epsilon = O(10^{-3})$) to ensure that inelastic events are not stimulated.

The process of imposing strain increments was repeated, each time using the newly minimized microstructure as a starting point to achieve a sequence of deformed microstructures. Deformation increments were imposed for each type, in all possible directions of the cell, for each of the 13 minimized 1.8-nm microstructures and on both of the minimized 3.0-nm microstructures obtained in II. In addition, the contribution of long-range nonbonded interactions was also considered to avoid truncation errors. Thus, a "tail correction" factor (described fully in section 4.0) that is inversely proportional to the volume is included in the potential energy of the system and has the following form:

$$U^{pot}_{tails} = \Delta U^{pot}_{tails,0}\left(\frac{V_0}{V}\right) \quad (8)$$

For PC microstructures with a starting cube edge length of 1.8 nm, $\Delta U^{pot}_{tails,0} = -22.6$ kcal/(mol of structures). An example of the simulation is shown in Figure 1, where the system potential energy, U^{pot}, is plotted as a function of uniaxial tensile strain for a pure uniaxial tensile simulation of a microstructure with a starting cube edge length of 1.8 nm.

For all of the deformations the second derivative of the system potential energy, U^{pot}, with respect to the specific types of ϵ discussed above, was obtained using a least squares fit method. From these calculations values for B, G, and c_{11} were obtained which were then used to find a set of Lamé constants that together as a set give the best values of the moduli.

4.0. Modeling of Large-Strain Plastic Deformations

4.1. Model Parameters. Amorphous PC microstructures that were generated by the modeling technique described in II were utilized. These represent static models of dense, disordered packings of density appropriate to a temperature of 300 K and of minimum potential energy characteristics described in II and summarized in section 3.0.

4.2. Atomic-Level Stress and Strain. For its central importance in our present study we recall the atomic site stress tensor, as generalized by Theodorou and Suter to include interatomic torques arising from bonded interaction:[4-6]

$$\sigma_{i,LM} = -\frac{1}{V_i}\sum_{j\neq i}^{\text{all atoms}}\left(r_{ij,L}F_{ij,M} + \sum_{K}^{\text{all bonded atoms}} e_{LMK}\frac{T_{ji,K}}{2}\right) \quad (9)$$

where $\sigma_{i,LM}$ is an element of the atomic stress tensor for atom i, V_i is the volume of the Voronoi polyhedron surrounding atom i, r_{ij} is the vector separating atoms i and j, F_{ij} is the sum of the bonded and nonbonded forces acting between atoms i and j, e_{LMK} is the permutation tensor,[31] and T_{ji} is the torque vector acting on atom j from i.[39] The force and torque balances for the PC repeat unit needed for this calculation follow essentially the scheme described in detail by Theodorou and Suter,[5] with the exception of the phenylene ring. The details of the force and torque balances, as related to the phenylene ring, considered as a rigid atom grouping, are given in Appendix A. The stress tensor for the entire system, σ^{sys}_{LM}, is a sum of all the individual stress tensors, weighted by their Voronoi volumes, i.e.

$$\sigma^{sys}_{LM} = \frac{1}{V}\sum_{i}^{\text{all atoms}} V_i\sigma_{i,LM} \quad (10)$$

where V is the total volume of the system.

Two scalar invariants of the stress tensor are of interest: the hydrostatic pressure, p, and the von Mises shear stress, τ:

$$p = -\mathrm{Tr}(\sigma)/3 = -{}^1/_3(\sigma_{11} + \sigma_{22} + \sigma_{33}) \quad (11)$$

$$\tau = \{\mathrm{Tr}(\sigma + p\mathbf{I})^2/2\}^{1/2}\{{}^1/_6[(\sigma_{11} - \sigma_{22})^2 + (\sigma_{22} - \sigma_{33})^2 + (\sigma_{33} - \sigma_{11})^2] + (\sigma_{12}{}^2 + \sigma_{13}{}^2 + \sigma_{23}{}^2)\}^{1/2} \quad (12)$$

where σ and $\mathbf{I}$ are the stress tensor and identity tensor, respectively.

On the atomic scale a positive atomic-level pressure indicates that the atom is in a compressed environment with a high coordination number. Correspondingly, the atomic von Mises shear stress on the site is a measure of the asymmetric distortion of the local environment.

To fully appreciate how strain is distributed at the atomic level, Mott, Argon, and Suter[32] have developed an atomic-level strain increment tensor. In this development the strain increment that an atom environment experiences is represented by determining first the deformation gradient tensor for each interstitial site between atoms

for each deformation increment, based upon the change in shape of all interstitial space, represented by a volume-filling set of Delauney tetrahedra. The strain increment of an atom environment is then constructed as the weighted volume average of the displacement gradients inside all the relevant Delauney tetrahedra that contribute to the volume of the Voronoi polyhedron surrounding an atom.

Two invariants of the atomic site strain increment tensor are utilized, the local dilatation increment $d\epsilon$ ($d(\Delta V/V)$) and the von Mises work equivalent shear strain increment $d\gamma$, defined as:

$$d\epsilon = \mathrm{Tr}(d\epsilon) = d\epsilon_{11} + d\epsilon_{22} + d\epsilon_{33} \tag{13}$$

$$d\gamma = \{2\mathrm{Tr}[d\epsilon - (d\epsilon \mathbf{I})/3]^2\}^{1/2} = \{^2/_3[(d\epsilon_{11} - d\epsilon_{22})^2 + (d\epsilon_{22} - d\epsilon_{33})^2 + (d\epsilon_{33} - d\epsilon_{11})^2] + 4(d\epsilon_{12}{}^2 + d\epsilon_{13}{}^2 + d\epsilon_{23}{}^2)\}^{1/2} \tag{14}$$

which are both in a work-conjugate association with the two invariants of the atomic-level stress tensor. In Equations 13 and 14 $d\epsilon$ is the strain increment tensor, while $d\epsilon$ is merely the dilatation increment. The dilatation is a measure of the relative change in volume about an atom, and the work equivalent shear strain increment $d\gamma$ is a measure of the incremental volume distortion. When the volume allotted to an atom increases, the dilatation is positive. The strain increment tensor for the entire system, $d\epsilon_{LM}^{sys}$, is a sum of all the individual strain increment tensors weighted by their volume fraction and is equal to the applied strain increment, $d\epsilon_{step}$:

$$d\epsilon_{LM}^{sys} = d\epsilon_{step} = \frac{1}{V}\sum_{i}^{\text{all atoms}} V_i\, d\epsilon_{i,LM} \tag{15}$$

4.3. Shear Deformation of the Microstructures. The methods for large-strain deformation of the microstructures that were developed by MAS[4] were used also in the present study. The system is deformed by first changing the continuation vectors that govern the periodicity of the system, according to the demands of the imposed strain increments. The energy of the system is then reminimized to reach a new equilibrated deformed state. For large-strain deformations, this process is done in a stepwise fashion, where at each step only a very small strain increment on the order of 10^{-3} is applied to the system to avoid convergence problems in the energy minimization. This procedure is repeated many times until the desired total strain is reached. Since time does not enter and there is no thermal activation, the rate of deformation is undefined.

In the pure shear simulation, at constant volume, the strain increments were applied to the borders in either the xy–xz or yz planes so that the continuation vectors remained orthogonal and the volume of the microstructure always remained constant. In this manner the energy minimization technique could be used unmodified with regards to the imposition of the periodic boundary conditions, and problems arising from symmetry breaking in the arrangement of the images of the parent chain are avoided. Thus, for shear in the xy plane, the imposed incremental strain was

$$d\epsilon_{step} = \begin{bmatrix} 1 & 0 & 0 \\ 0 & -1 & 0 \\ 0 & 0 & 0 \end{bmatrix} \times 10^{-3} \tag{16}$$

to first-order quantities.[40]

Three microstructures with original cube edge lengths of 1.844 nm were chosen to be deformed. Of these, two were the same that were used for the chain dynamics studies reported earlier;[3] the third microstructure was randomly chosen. For each chosen microstructure, deformations were imposed in all three of the above-mentioned planes, and for one microstructure the deformation was imposed in both the positive and negative directions, making up a total of 12 separate simulations. One hundred strain steps were applied for each simulation, with each step representing 0.2% work equivalent shear strain. The resulting total equivalent strain imposed on the system was 20%.

Table I
Comparison of Experimental and Predicted Values of the Elastic Constants

property	exp range[a]	pred value (±SE[b])
Lamé const, λ, MPa	4270–5550	5350 ± 1150
Lamé const, μ, MPa	800–1100	2060 ± 650
G, MPa	800–1100	2060 ± 650
E, MPa	2300–2500	5600 ± 1700
B, MPa	5000–6100	6700 ± 1600
ν	0.42–0.43	0.36 ± 0.06

[a] References 33 and 34. [b] SE = standard error.

5.0. Results and Discussion

5.1. Small-Strain Elastic Constants. There was considerable scatter in the values of the elastic constants calculated for a given deformation from microstructure to microstructure and in different directions for an individual microstructure. For the 3.0-nm microstructures, since there were only two specimens to work with, the scatter proved to be too large to obtain reasonable results. The average values (±standard error) obtained from the deformation of the 13 smaller structures (undeformed cube edge length of 1.8 nm) are listed below, where the results for the tension and the shear deformations are averaged over all directions and over all the microstructures:

uniaxial tension

$$(1/3)(c_{11} + c_{22} + c_{33}) = 8610\ (\pm 1826)\ \text{MPa} = 2\mu + \lambda \tag{17a}$$

shear

$$(1/3)(c_{44} + c_{55} + c_{66}) = 3212\ (\pm 2139)\ \text{MPa} = \mu \tag{17b}$$

bulk compression

$$B = 7588\ (\pm 2291)\ \text{MPa} = \lambda + (2/3)\mu \tag{17c}$$

From the relations given in eqs 3a–c, the Lamé constants obtained using any two values of eqs 17a–c can be used to calculate the third value. The values of G calculated using c_{11} and B are widely different, indicating that the ensemble of microstructures did not respond as an isotropic solid to small elastic deformations. The best-fit values of λ and μ and the moduli calculated with them are compared with experimental values in Table I.

When compared with the experimental moduli,[33,34] all the calculated best-fitting values of the moduli fall well above the reported experimental range, indicating that the ensemble of small microstructures is too "stiff" in its response to deformation. Calculations using the Lamé constants obtained with the average values of the moduli indicate that it is the response of the ensemble to the shear deformation which is much too stiff. These results are in contrast with the results for PP calculated by Theodorou and Suter in which the predicted moduli were within 15% of the experimental values.[5] A possible explanation for the overestimation of the moduli is that the rigid segments of the PC molecule are larger and have

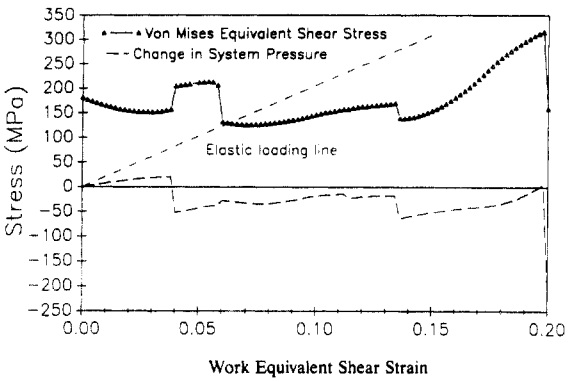

Figure 2. Stress vs strain response for a pure shear simulation. Plotted are the work equivalent shear strain vs the von Mises shear stress and the change in the hydrostatic pressure. The elastic loading line represents the behavior of a perfectly elastic solid in shear with the same microscopic modulus.

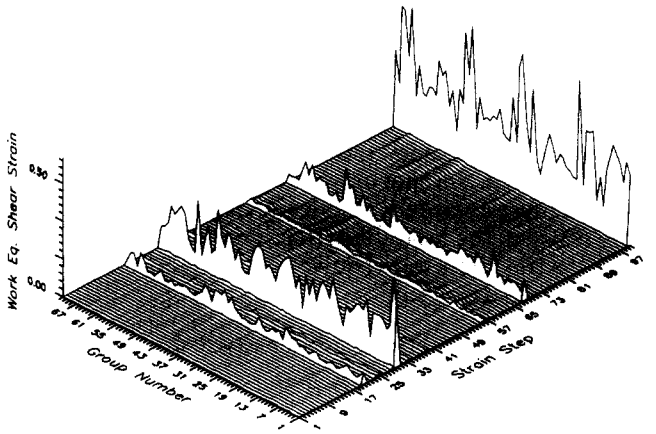

Figure 3. Distribution of the atomic-level increments of the work equivalent shear strain occurring in each external strain increment at all the backbone atom group positions along the chain, calculated for the simulation shown in Figure 2.

fewer degrees of freedom per unit volume than PP, and therefore the size of the simulation cells is more limiting for PC than PP. However, the deviation of the predicted values from the experimental mean value given in Table I is less than 2 standard errors in every case, so that agreement with experiment is still quite satisfying.

5.2. Stress–Strain Responses of Individual Microstructures. The stress vs strain response from one of the 12 pure shear simulations of individual microstructures is shown in Figure 2. The figure shows the dependence of the von Mises shear stress and the system pressure on the integrated total work equivalent shear strain. Here the von Mises shear stress on the system is obtained by first obtaining the total stress tensor on the whole system by the weighted volume average of the atomic-level stress tensors, followed by the determination of the second invariant of this total stress tensor. The system pressure, plotted in Figure 2, is the total pressure increment with respect to the pressure of the initial state. The elastic loading line represents the behavior of a perfectly linear elastic solid with elastic moduli determined from Table I. The behavior found in this figure is characteristic of the wide variations that can be found in the simulations and is in many ways very similar to the deformation results on PP reported by MAS.[4] The feature common to all the individual microstructure simulations is that the initial von Mises shear stresses are nonzero and high in the small systems and that the change in stress is smooth in general in the early phases of deformation, with large jumps in the von Mises stress and pressure occurring at varying intervals and amplitude in the later stages. No clear elastic to plastic transition could be found in the individual microstructure simulations, which are all characterized by a soft reversible behavior that is only gradually "sheared out" of the system and is replaced by a succession of much better defined linear reversible loading steps terminated by irreversible rearrangements associated with the stress jumps.

The large initial stresses of the undeformed microstructures show that the systems chosen have high residual von Mises stresses on the order of 200 MPa over the simulation cell. Indeed, upon inspection of all 13 1.8-nm microstructures, it was found that they all had residual von Mises stresses of about the same level. This is a consequence of the very large magnitudes of the random atomic-level stresses present in the initial state of the system. In the present study the disorder-related atomic-level stresses of the undeformed microstructures were found to be in the range of 10 GPa and quite similar to those calculated for PP.[6] Since the system stress is a volume-weighted sum of these atomic-level stresses, in the small systems the random sum of these stresses in the initial undeformed state does not average to zero and a substantial residue remains. This effect has been termed an atomic-level "stress noise" by MAS. A much larger system would be required to obtain residual stresses close to zero since the average random sum stresses decrease only with the square root of the number of atoms in the system.[4]

In the areas where the stress variation is continuous, the conformational changes occurring in the microstructures were found to be reversible upon reversal of the deformation. However during the sharp drops or increases in stress, the conformational changes were irreversible and reversal of the deformation after a stress jump did not cause a reverse jump. The early stages of deformation are anelastic and the slopes are less than the slope of the elastic loading line, while in the later stages the slopes of the lines between discontinuous stress drops are more closely parallel to the elastic loading line, the slope of which was obtained using the value of 2060 MPa for the shear modulus that was determined in section 5.1. While this was the trend, the majority of the time, however, the slopes were somewhat different from the slopes of the elastic loading lines, consistent with expectations that individual states of microstructures are far from being isotropic. In general, the greater the slope before a stress jump, the larger was the magnitude of the jump. During the stress jumps the microstructure undergoes a far-reaching irreversible *plastic* rearrangement which we will discuss below.

Since the simulations were performed at constant volume, the pressure change during the deformation should also be zero if the microstructures were behaving as isotropic, nondilating plastic solids. The pressure changes occurring in the microstructures were, however, rarely zero as the typical case of Figure 2 shows. The general trend shown in Figure 2 is a gradual rise in pressure accompanying the reversible, soft anelastic behavior and a drop in this built-up pressure accompanying a sharp plastic relaxation step. This behavior parallels what was found by MAS for PP.[4]

An important feature of these simulations involves the detailed examination of the local atomic-level processes by both graphical and direct visual means. The calculation of the atomic-level strain increment tensor for the simulation shows that during the abrupt plastic events there is a large amount of relative segmental movement occurring in the entire structure. Figure 3 shows the changes in the atomic-level strains for the simulation of Figure 2. The figure shows the spatial and sequential distribution of the

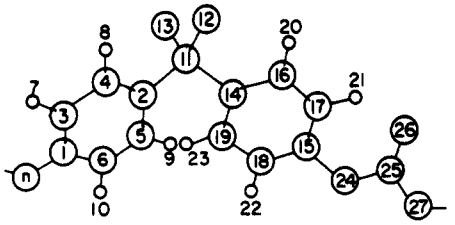

Figure 4. PC repeat unit and the numbering scheme of atom groups.

work equivalent shear strain increments plotted for each of the more than 70 atom groups along the chain as a function of strain step. Here the atomic-level strains have been summed together for atoms of internally rigid molecular groups that can have no significant relative displacement between each other, due to the rigid bond angles and bond lengths that connect them together, such as the phenylene ring. Thus, referring to Figure 4, which shows the PC repeat unit and its numbering scheme, atoms 1–10 were treated together to represent the strain of the first phenylene ring of the repeat unit and atoms 14–23 were similarly treated together for the second ring. Atoms 11–13 make up the isopropylidene group, and atoms 24–27 are considered together as a unit for the strain compilation for the carbonate group. Thus, these groups are treated as internally rigid. Therefore, a total of three different types of groups make up the entire chain.

Upon inspection of Figures 2 and 3 together, it can be seen that during the reversible portions of the deformation, very little relative movement of the molecular groups is occurring. However, during the abrupt plastic events, a great deal of movement occurs at nearly every atom group which is largely proportional to the size of the corresponding stress jump. The dilatation occurring during each strain increment, which is not shown here, demonstrates the same behavior. The large strains that are present during these plastic events correspond to relatively more substantial structural changes that are happening in the system in which the environment of *every* atom or atom group of the chain is altered. This behavior where every part of the chain moves during these plastic straining events is again very similar to that found in PP. As in the case of the PP simulation of MAS, stereo pairs of many changing conformational states were prepared and examined visually in great detail to detect recurring elementary kinematical components of conformational alterations during the irreversible rearrangements. As we will discuss in section 5.5, none could be reliably recognized.

The simulations show that in the regions of elastic loading between plastic events there must be a buildup of elastic strain energy which is then dissipated during the plastic events.[4] While the internal energy of the system always increases during the elastic regions of the deformation, it decreases or stays nearly constant during the plastic strain events, even though the overall stress of the system during these events can either increase or decrease. It is necessary that during the abrupt irreversible changes the Gibbs free energy of the system must always decrease as verified by Deng et al.[14] and also by MAS for the PP simulation. This is expected to hold true for the irreversible events in the present study as well.

5.3. Ensemble-Average Stress–Strain Response. The ensemble-average stress–strain response of the 12 individual deformation simulations is shown in Figure 5. Among the features to be noted is that the initial stress level is now much lower for the ensemble average than for the individual microstructures although it is still not negligible. The portion of the curve with a low initial

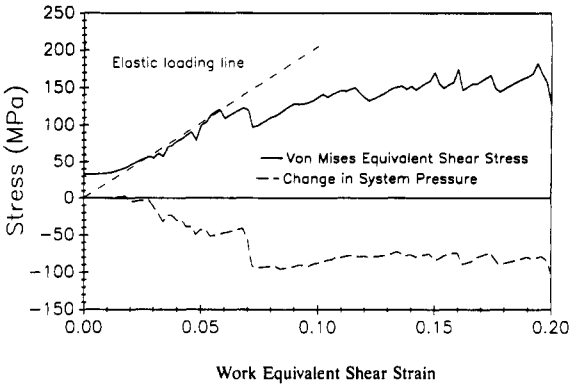

Figure 5. Ensemble-average stress–strain response of the 12 pure shear deformations.

slope signifying anelastic behavior is now limited to only 1.5% strain and then increases to become parallel to the elastic loading line. The region with the small initial slope and the considerable atomic-level stress "noise" should monotonically decrease further with increasing numbers of simulations in an inverse dependence on the square root of the total number of atom groups in the simulations or with the number of such simulations. Despite the "noise" and the weak stress jumps, the stress response increases nearly linearly at a constant slope parallel to the elastic loading line up to about 6–7% strain, where the slope then decreases markedly and eventually flattens out to become, on the average, nearly parallel to the strain axis.

This stress–strain behavior of PC is similar to that of PP. However, the behavior of the change in pressure of the ensemble for PC contrasts starkly in comparison with the behavior of PP. For PP, there was a systematic buildup of pressure during the deformation, indicating that the system was dilating during its early stages of reversible flexing. Inspection of Figure 5 shows that in PC the pressure stays nearly constant up to about 2% strain, and then it monotonically decreases up to about 7% shear strain, where it levels off at a value *less* than the initial value of the ensemble. This demonstrates that the system has a distinct tendency to contract, or get denser, upon plastic deformation. This is in agreement with experiments of Wu[35] and Brady and Yeh,[36] who found that the density of PC increases after undergoing plastic shearing. The nature of deformation-induced structural conformational polarization that results in this compaction is not yet clear. A possible explanation is given at the end of the following section.

5.4. Size of Local Shear Transformations. It was already deduced from the widespread quasi-homogeneous distribution of atomic-level shear strain increments of Figure 3 that the microstructures were too small to show any localized isolated segment clusters undergoing plastic relaxations in an elastic background. A clearer conclusion can be reached by studying the stress jumps that occur in the individual deformation simulations, with the aid of which the size of the volume elements undergoing plastic flow can be estimated. Following the development of Argon and Bessonov[37] and MAS,[4] the volume Ω of the region undergoing a coherent plastic transformation, entirely surrounded by an elastic region, can be deduced from the experimentally determined shear activation volume, V^*, which is defined as

$$V^* = \left(-\frac{\partial \Delta G^*}{\partial \tau}\right)_{p,T} = \Omega \Delta\gamma^* \qquad (18)$$

where ΔG^* is the activation free energy and $\Delta\gamma^*$ is the

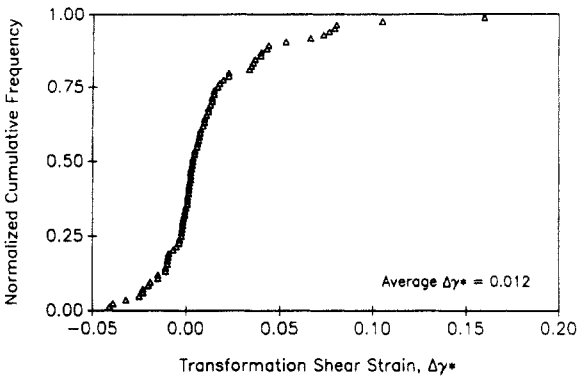

Figure 6. Cumulative distribution of the transformation shear strains $\Delta\gamma^*$, recorded at the main irreversible plastic rearrangements.

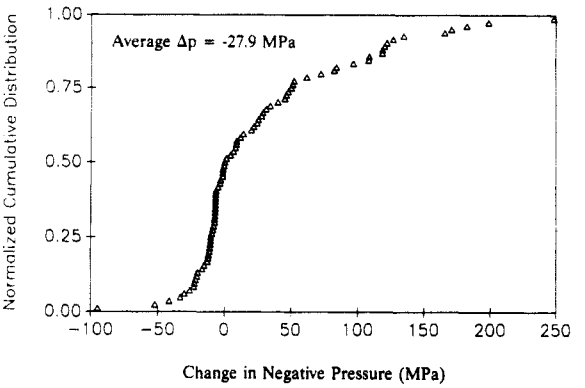

Figure 7. Cumulative distribution of the change in the hydrostatic pressure that accompanies the irreversible plastic shear events.

transformation shear strain in the region of volume Ω undergoing the coherent plastic relaxation.

Operationally, the activation volume can be obtained from strain rate change experiments during plastic shearing via the expression

$$V^* = kT\left(\frac{\partial \ln \dot{\gamma}}{\partial \tau}\right)_{p,T} \tag{19}$$

where τ is the shear stress and $\dot{\gamma}$ is the shear strain rate. A very good measure of the transformation shear strain, $\Delta\gamma^*$, can be obtained from the simulations using the stress jumps resulting from plastic relaxations under conditions of zero total strain when elastic strain is converted to irreversible plastic strain, giving

$$\Delta\gamma^* = -\Delta\tau/G \tag{20}$$

where $-\Delta\tau$ is the magnitude of the shear stress drop and G is the average shear modulus. The cumulative distribution of the $\Delta\gamma^*$ that were determined by this procedure is shown in Figure 6, where a drop in the corresponding stress is considered to lead to a positive transformation shear strain as eq 19 indicates. The activation volume of PC has been measured experimentally by Argon and Bessonov[37] to be 6.47 nm^3. Using 1.2% for $\Delta\gamma^*$ as the average value of the distribution of $\Delta\gamma^*$, the corresponding volume Ω was found to be 539 nm^3. This indicates that the diameter of the shear transformation is of the order of 10.1 nm, assuming Ω is of roughly spherical shape. It can therefore be concluded that cooperative motion of several hundred chain segments is involved in a coherent plastic shear transformation. This contrasts sharply with previous depictions of the plastic flow units in which much larger transformation shear strains among much smaller and localized chain elements have usually been assumed. Our value of 1.2% for the plastic shear strain is very closely similar to the value of 1.5% calculated by MAS for PP, indicating that the resulting shear transformation volumes for PC are also of similar magnitude as those in PP.

The change in the system pressure that accompanies these abrupt plastic relaxations provides additional insight into their nature. The distribution of the magnitudes of the system pressure changes is displayed in Figure 7. The figure shows that while positive and negative pressure changes were nearly equally likely, the magnitudes of the negative pressure changes were, on the average, larger than the pressure changes over the range of straining (i.e., 0.2) explored in the simulation, resulting in an average *negative pressure* change of 27.9 MPa for the plastic events over the extent of the simulation. As Figure 5 shows, in the early stages of deformation the material is becoming denser upon shearing. Clearly, during steady-state shearing at large strains the density cannot continue to increase. Then the pressure changes during plastic rearrangements partition more equally between positive and negative values. As an accompaniment to the interpretation of the drops in shear stress as reflecting the magnitudes of the transformation shear strain of plastic rearrangements, it is possible to associate the pressure changes with an accompanying transformation dilatation by dividing the pressure change with the average bulk modulus $B = 6.7$ GPa. This gives an average transformation dilatation of $\Delta\epsilon^* = -4.2 \times 10^{-3}$ that is influenced more heavily by the processes occurring in the early phases of deformation, as already remarked above. The above behavior of PC contrasts markedly with the behavior of PP, where a buildup rather than a decrease of system pressure resulted from the elastic flexure of the plastic deformation units in the material, indicating that in PP the system expands during reversible elastic flexure but on the average undergoes only a negligible volume change during the irreversible plastic relaxations. It is likely that this difference in the shear-induced pressure response between PP and PC is a result of the far less structured form of the PP molecule than the PC molecule, suggesting that the several relatively rigid atomic groupings in PC which are initially packed randomly find it possible to settle into lower energy forms upon shearing.

5.5. Kinematics of Chain Motion during Plastic Events. In PP, MAS found it difficult to identify any recurring specific chain segment motions that contributed more than the average to the plastic events. This was partially due to the simplicity of the PP repeat unit, which is relatively structureless and has few distinguishing features or conformations of the chain. The situation is different for PC. The rotation of phenylene rings and the conformational changes of the carbonate group are known to give rise to specific stress relaxations and can be easily investigated, as was demonstrated by us earlier.[3] In that previous study, the phenylene ring rotation and the carbonate group conformational change were imposed on the system, and it was the response of the system to this perturbation that was studied. Thus, in the case of plastic deformation, it should be interesting to investigate how shear perturbations *on the system* may or may not induce such rotations or conformational changes. Figures 8–10 show the local work equivalent shear strain felt by the individual molecular groups during the plastic events of the simulation featured in Figure 3. In Figure 8 the work equivalent shear strain experienced by specific phenylene rings during plastic relaxation events is plotted against the rotation of these phenylene rings. The local work equivalent shear strain vs the change of the carbonate group orientation is depicted in turn in Figure 9. Finally, the local work equivalent shear strain vs the rotation in

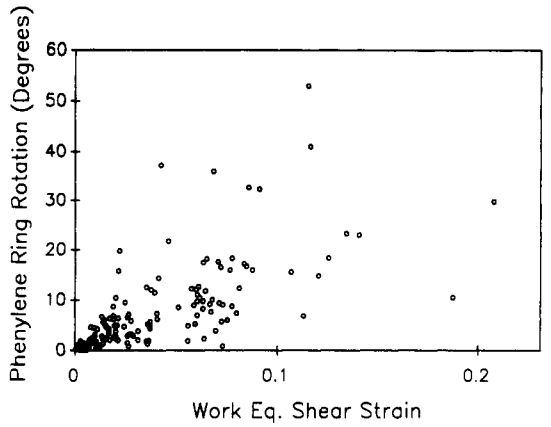

Figure 8. Association of the phenylene ring rotations with the local increments of the work equivalent shear strain at all ring sites during the irreversible plastic shear events. Rotation is defined as the angle between the normal vectors to the phenylene ring.

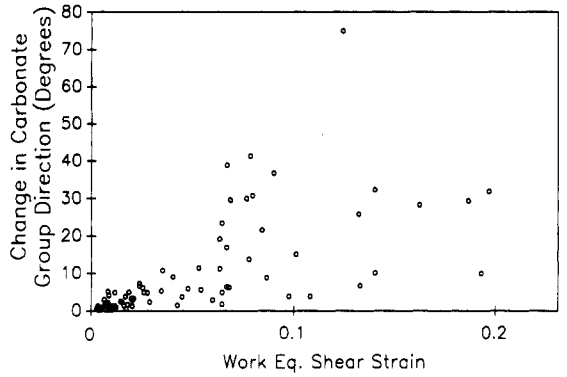

Figure 9. Association of the carbonate group reorientations with the local increments of the work equivalent shear strain at all carbonate group sites during the irreversible plastic shear events. Group reorientation is defined as the angle between the vectors along the C=O bond in the carbonate moiety.

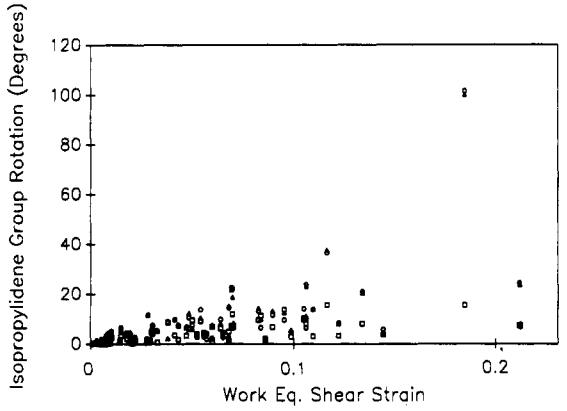

Figure 10. Association of the isopropylidene group reorientations with the local increments of the work equivalent shear strain at all isopropylidene group sites during the irreversible plastic shear events. The open squares represent the change of the plane containing the C_{ar}–sp^3 C–C_{ar} bond, the open circles represent the change in the plane containing the methyl–sp^3 C–methyl bonds, and the open triangles represent the change of the plane normal to the above two mentioned planes.

the planes of the isopropylidene groups is featured in Figure 10, where the different symbols indicate the change in the different planes of the group. Therefore, what is represented in these figures is the occurrences of the specific chain motions that take place during the shear transformation inside a specific plastically relaxing volume Ω. First, it can be seen that the imposed deformation does indeed induce ring rotations of considerable magnitude, with a few being between 30 and 50°. The carbonate groups and the isopropylidene groups also undergo substantial reorientations during the plastic events. This gives an indication of the magnitude of the main-chain motion (the largest reorientation of over 100° of an isopropylidene group occurred during the last and largest plastic event shown in Figure 3 to an isopropylidene group close to that chain end). From here we can conclude that these various well-defined motions are induced during the plastic rearrangements of the polymer and are all more or less kinematically necessary as the internal make-up of the plastically relaxing element Ω.

The second feature that can be deduced from Figures 8–10 is that there is only a very weak correlation between the strain felt by a molecular group and the magnitude of the rotation of that group. If there was no correlation, the data points in the figures would be randomly spread across the whole plot, which is not the case. There are clusters about the origins of all three plots, demonstrating that the groups that feel smaller amounts of strain move less. However, those groups that feel large amounts of strain do not necessarily show large reorientational movements. It is suggested from Figures 9 and 10 that the carbonate groups and the isopropylidene groups that feel small strains do not undergo large rotations or reorientations.

While rotations of individual groups are attractive to monitor and are clearly both kinematically necessary and directly associated with shear strain, the converse is not true; i.e., isolated rotations of volume elements do not produce shear strain. The association of rotation of a group and the shear strain that it suffers is often complex—particularly in the context of our simulation. Therefore, a more direct approach of determining the contribution of each group to the overall shear and establishing its correlation to the accompanying rotation should be of interest.

By studying the volume fraction occupied by certain molecular groups and the corresponding strain fraction felt by those groups, it is possible to infer how the groups are participating relative to each other in the plastic flow. Figures 11a–e shows the volume fraction calculated using the van der Waals radii, the volume fractions of groups calculated using the Voronoi polyhedra, and the strain fraction of the featured molecular group for the entire simulation shown in Figures 2 and 3. The strain fraction is the work equivalent shear strain felt by those particular molecular groups normalized with respect to the total work equivalent shear strain of the chain. The volume fractions calculated using the van der Waals radii should of course remain constant throughout the simulation. The volume fractions calculated using the Voronoi polyhedra should also remain relatively constant but should be subject to some alterations as the local environments of the groups change. As the figures show, the expectations are correct and the two volume fractions measured are very close. This indicates that the volume occupied and the surroundings of the specific molecular groups, as measured with the Voronoi polyhedra, correspond closely to the sum of the atoms of the associated molecular group and do not change significantly upon deformation.

Whereas the Voronoi volume fraction of the groups stays nearly constant during the simulation, as it must, the strain fraction of the groups varies widely. First, the strain fraction felt by a particular type of molecular group does not completely correspond to the volume associated with that group. Clearly, the isopropylidene groups and the carbonate groups undergo more strain relative to their volume occupied, and the phenylene rings undergo less

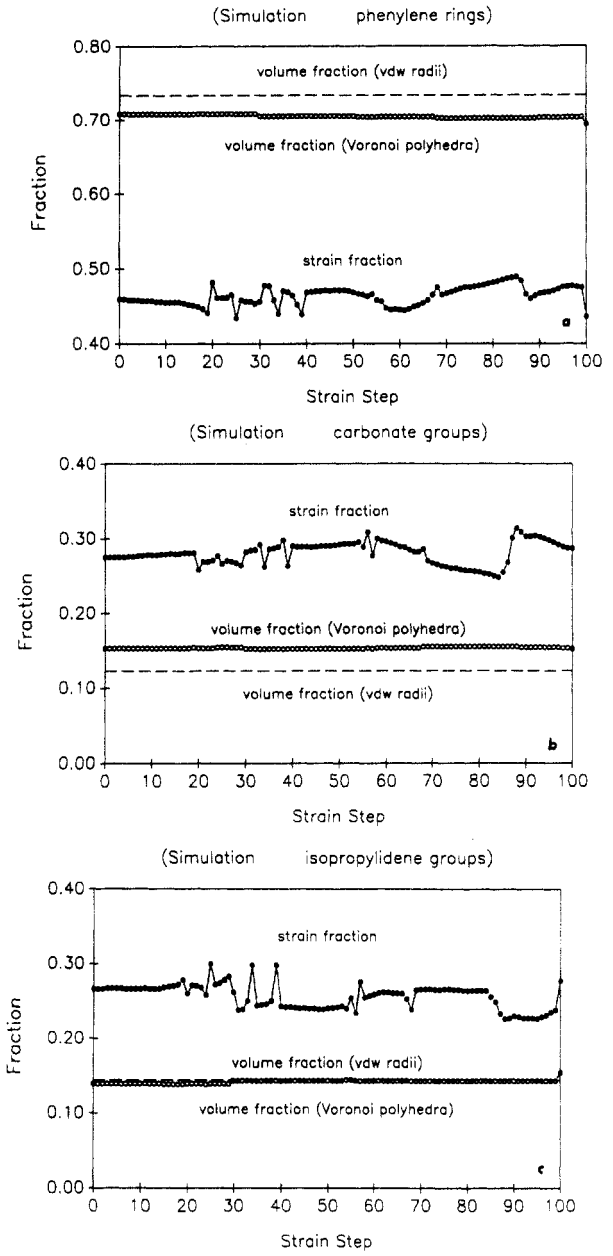

Figure 11. Volume fractions calculated using the van der Waals radii and using the Voronoi polyhedra and the strain fraction for the (a) phenylene rings, (b) carbonate groups, and (c) isopropylidene groups for the entire simulation shown in Figures 2 and 3.

strain relative to their volume; i.e., the isopropylidene group and the carbonate groups tend to contribute more to the overall strain, while the phenylene rings contribute less, in keeping with the largely rotational response of the latter. In addition, the strain fractions of all the types of molecular groups change during the deformation, not just during the plastic events but also during the anelastic response regions. This suggests that the task of strain production is being transferred from group to group not only during the plastic events where there is a large amount of relative atomic movement but also during the anelastic regions where the atomic movement is very small. This conclusion is already apparent in Figure 3, which shows large differences in the individual groups in their capacity to contribute strain to the overall assembly during an irreversible plastic event.

Since simple group rotations have been successfully associated with specific relaxations or internal friction peaks in many glassy polymers, there has been a general expectation that large-strain plastic flow can also be explained simply by such rotations—albeit in greater concentration. Thus, e.g., the notion is widespread that the impact toughness of certain polymers, and, more specifically, PC, is a direct consequence of a prominent β relaxation that this polymer exhibits at low temperatures. This is in spite of the fact that it is well known that toughness or brittleness in glassy polymers is a direct consequence of other intermediate-scale phenomena such as the propensity of a polymer for crazing and the many processes that govern the mechanical stability of craze matter. Our present simulation of plastic straining of PC and our previous study[3] of the energetics of phenylene ring rotations and carbonate group rearrangements in this material demonstrate directly the tenuous nature of this association. Our previous study[3] has demonstrated that simulation could give accurate results for the activation energies of phenylene ring rotations and carbonate group rearrangements which compare well with experimental measurements such as NMR etc. Moreover, the fact that such rotations are directly linked to low-temperature internal friction peaks through the local anelastic relaxations that they permit is well established. Our present simulation has demonstrated that these specific processes also occur during irreversible plastic relaxations but that they occur collectively together with other more diffuse conformational rearrangements in a very large molecular cluster, involving a large collection of local groups. Thus, these specific processes appear as kinematically necessary ingredients of the transformation strain in the overall cluster. In fact, Figures 11a–c show that the rotation of phenylene rings contribute less to the overall local strain in the cluster than, e.g., carbonate group and isopropylidene group rearrangements contribute. Apart from the more structured nature of the PC molecule that permits better monitoring the activity in specific groups, the picture of local plastic strain production in the collective action of large clusters is nearly identical to what MAS have observed in their simulation of plastic strain in PP.

It is now necessary to radically revise notions of plastic flow mechanisms in glassy polymers. The simulation of MAS and our present simulation demonstrate clearly that because of the inextensional nature of the backbone primary bonds and the relatively inflexible nature of primary bond angles, conformational rearrangements in chain molecules of a glassy polymer can occur primarily only by torsional rotations along the chain backbone. This imposes severe constraints on the development of a transformation shear strain in a cluster that is to undergo a coherent plastic relaxation and necessitates a collective action in a very large group of molecular segments that is estimated to be typically of a diameter in the range of 8.0 nm, in both PP and PC. The simulations have shown that the transformation shear strains of typical magnitudes of 1.2–1.5% in a fully dense glassy polymer are accommodated by a series of small but highly cooperative conformational adjustments that to all forms of direct examination appear chaotic. Nevertheless, since the irreversible plastic relaxations are discrete and very sharply defined events, it must be concluded that the very large numbers of degrees of freedom in the cluster must be nearly fully constrained, leaving only *one* effective degree of freedom for the cluster to transit over the saddle point of the potential contours, from the ground state to the plastically fully relaxed new state in our (effective 0 K) simulation. Clearly, if our model had incorporated thermal motions explicitly, additional configurational paths over the saddle point would have become available and the actual response would have been less jagged and smoother.

In addition, thermal fluctuations, by helping the system to overcome the potential barriers under smaller stress, would have smoothed out the "spikes" in the shear strain curves.

The results of our simulations and our conclusions are strongly governed by considering no important bond extension and bond angle change flexibility and attributing all conformational rearrangements to only the torsional degrees of freedom. Considering the very large (by order of magnitude) differences in the resistance to bond extension and angle flexing on the one hand and the torsional rotations on the other, the assumptions of our model are justified and the conclusions derived from the model should be valid. This conclusion is strengthened from a molecular dynamics study of Sylvester et al.[38] of the changes in molecular segment mobility at the glass transition in PP, where realistic harmonic potentials were incorporated for bond length and bond angle changes. This study showed that the introduction of these new degrees of freedom over the torsional degrees of freedom resulted only in marginal changes in the system to undergo conformation changes. Nevertheless, introduction of these in a broadened study of the shear response should produce some quantitative but no qualitative changes in our conclusions.

The above notions of highly constrained molecular motions in dense glassy polymers is quantitatively different from the corresponding processes in atomic glasses studied by Deng et al.,[14] where cooperatively rearranging plastic clusters were much smaller due to the absence of chain constraints and the role of an available excess volume per atom (free volume) was much more readily assessable. The simulations of Sylvester et al.[38] of the kinematics of molecular mobility at or around a glass transition in PP also support the present realization that in a fully dense glassy polymer the increased molecular motions above a glass transition are of a very cooperative nature and less readily associated with local excess volume than is the case of atomic glasses.

6.0. Conclusions

Although the simulation results for the elastic moduli are consistently higher than the experimental range, the predicted results are in broad agreement with experiment. The overestimation of the elastic moduli could be caused by several factors, the primary one, most probably, being the small size of the simulation cell.

The simulation of the large-strain deformation of glassy PC has clarified a number of previously ill-understood aspects of plastic deformation in glassy polymers. The deformation behavior of the individual microstructures includes early regions in the stress–strain curves where the response of the material is "soft" and anelastic and where there is little far-reaching relative atomic movement. In later stages of deformation large stress jumps or "plastic events" were found where there is far-reaching relative atomic movement. The ensemble-average stress–strain curves show much less soft behavior and give a response that is nearly parallel to the elastic loading line from almost the beginning up to a shear strain of about 6–7%. Beyond this strain the polymer deforms at relatively constant (flow) stress, indicating well-developed plastic behavior. The large-strain response of the ensemble shows a decrease in system pressure with increasing strain, indicating that the initial glassy material has a strong tendency to become denser, and perhaps more ordered, upon deformation. By measuring the pressure changes associated with the plastic events, it could be shown that the plastic response of the material is at least partly responsible for the pressure decrease that occurs during the deformation. This is in contrast to a general increase of pressure accompanying inception of plastic straining in PP, where the deformation is dilatant in the process of reaching a steady state.

The large-strain deformation of PC consists of a series of reversible elastic loading events followed by discrete irreversible plastic relaxations producing large drops in the von Mises shear resistance. Analysis of these stress drops as a collection of plastic shear transformantions has shown that the average value of the transformation shear strain in PC is 1.2%. This, when compared with the experimentally measured shear activation volumes, implies that the size of the cluster that is undergoing a coherent plastic relaxation, if considered as a spherical region, is roughly 8.0 nm in diameter involving complex cooperative motion of a very large number of molecular segments. This behavior compares very well with the results of similar simulations performed by Mott et al.[4] on PP where the transformation shear strain was found to be 1.5% and the volume of almost identical dimensions.

Analysis of the individual group motions in the plastic relaxation events indicated distinct recognizable rotations and movements in the phenylene rings, carbonate groups, and isopropylidene groups. It was found, however, that while these movements were readily identifiable and often of large magnitudes, they contributed to the overall strain collectively in a complex manner, indicating that they were kinematically necessary components of the transformation strain. It was found, e.g., that in the overall balance, rotation of phenylene rings on the average contributed less to the total strain than rearrangements in the carbonate and isopropylidene groups.

Acknowledgment. This research was supported by the Defense Advanced Research Projects Agency through the Office of Naval Research under Contract N00014-86-K-0768. M.H. was a member of the Program in Polymer Science and Technology at MIT. We thank Dr. P. H. Mott and Prof. M. F. Sylvester for many helpful discussions and also Dr. F. T. Gentile with aiding in the energy minimizations.

Appendix A

The repeat unit of PC and a sample numbering scheme for a phenylene ring are shown in Figure 3. The first ring of the repeat unit will be used as an example here, where atom n is the last atom of the preceding repeat unit. The bonded force and torque balances for each bond follow the method described by Theodorou and Suter,[5] where F^{NB}_i is the total nonbonded force acting on atom i, F^{B}_{ij} is the bonded force acting on atom i from atom j, and T^{B}_{ij} is the torque acting on atom i from atom j through the bond i–j. For the system to be in mechanical equilibrium, the following must be true for all atoms and all bonds:

$$\sum F = 0, \quad \sum T = 0 \tag{A.1}$$

The balances for all the atoms and bonds are straightforward, except that special consideration is needed for the "internal" bonds of the phenylene ring. Mechanically, the hexagonal structure of the phenylene ring is statically indeterminate, and the complete forces and torques acting on and between the carbon atoms of the ring (atoms 1–6) cannot be determined in the conventional way but required knowledge of interactions between atoms in the ring. The forces and torques between the carbon atoms, however, are internally in equilibrium and since they contribute little by themselves to the overall stress on the structure,

they can be lumped together and considered as a rigid group. This leaves the task of finding the bonded forces and torquies acting on the ring from the rest of the chain through the bonds (atom n to carbon 1) and (carbon 2 to atom 11). If the force and torque balancing was started in a bond by bond fashion from the left-hand end of the chain shown, the forces and torques leading into the ring, $F^{B}_{1,n}$ and $T^{B}_{n,1}$ would be known. The force and torque acting along bond (carbon 2 to atom 11) are unknown and can be found using a force and torque balance for the ring as a whole, i.e.

$$\mathbf{F}^{B}_{1,n} + \mathbf{F}^{B}_{2,11} + \sum_{i=1}^{10} \mathbf{F}^{NB}_{i} = 0 \qquad \text{(A.2)}$$

$$\sum_{i=1}^{10}[(\mathbf{r}_i - \mathbf{r}_2) \times \mathbf{F}^{NB}_{i}] - [(\mathbf{r}_n - \mathbf{r}_2) \times \mathbf{F}^{B}_{n,1}] - \mathbf{T}^{B}_{n,1} + \mathbf{T}^{B}_{2,11} = 0 \qquad \text{(A.3)}$$

Using the above balances, it is possible to obtain $F^{B}_{2,11}$ and $T^{B}_{2,11}$.

References and Notes

(1) Hutnik, M.; Argon, A. S.; Suter, U. W. *Macromolecules* **1991**, *24*, 5956.
(2) Hutnik, M.; Gentile, F. T.; Ludovice, P. J.; Argon, A. S.; Suter, U. W. *Macromolecules* **1991**, *24*, 5962.
(3) Hutnik, M.; Argon, A. S.; Suter, U. W. *Macromolecules* **1991**, *24*, 5970.
(4) Mott, P. H.; Argon, A. S.; Suter, U. W. *Philos. Mag.*, in press.
(5) Theodorou, D. N.; Suter, U. W. *Macromolecules* **1986**, *19*, 139.
(6) Theodorou, D. N.; Suter, U. W. *Macromolecules* **1986**, *19*, 379.
(7) Parrinello, M.; Rahman, A. *J. Chem. Phys.* **1982**, *76*, 2662.
(8) Sprik, M.; Impey, R. W.; Klein, M. L. *Phys. Rev.* **1984**, *29B*, 4368.
(9) Ray, J. R.; Moody, M. C.; Rahman, A. *Phys. Rev.* **1985**, *32B*, 733.
(10) Ray, J. R.; Moody, M. C.; Rahman, A. *Phys. Rev.* **1986**, *33B*, 895.
(11) Lutsko, J. F. *J. Appl. Phys.* **1988**, *64*, 1152.
(12) Maeda, K.; Takeuchi, S. *Philos. Mag. A* **1981**, *44*, 643.
(13) Srolovitz, D.; Vitek, V.; Egami, T. *Acta Metall.* **1983**, *31*, 335.
(14) Deng, D.; Argon, A. S.; Yip, S. *Philos. Trans. R. Soc. London* **1989**, *A329*, 613.
(15) Maeda, K.; Takeuchi, S. *J. Phys. F* **1982**, *12*, 2767.
(16) Tashiro, K.; Kobayashi, M.; Tadokoro, H. *Macromolecules* **1977**, *10*, 413.
(17) Tashiro, K.; Kobayashi, M.; Tadokoro, H. *Macromolecules* **1978**, *11*, 908.
(18) Clarke, J. H. R.; Brown, D. *Mol. Sim.* **1989**, *3*, 27.
(19) Weiner, J. H. *Statistical Mechanics of Elasticity*; Wiley: New York, 1983.
(20) Jansson, J.-F.; Yannas, I. V. *J. Polym. Sci., Polym. Phys. Ed.* **1977**, *15*, 2103.
(21) Lunn, A. C.; Yannas, I. V. *J. Polym. Sci., Polym. Phys. Ed.* **1972**, *10*, 2189.
(22) Robertson, R. *J. Chem. Phys.* **1966**, *44*, 3950.
(23) Argon, A. S. *Philos. Mag.* **1973**, *28*, 839.
(24) Yannas, I. V. *Proc. Int. Symp. Macromol.* **1975**, 265. Yannas, I. V.; Luise, R. R. In *The Strength and Stiffness of Polymers*; Zachariades, A. E., Porter, R. S., Eds.; Marcel Dekker: New York, 1983.
(25) Oleynik, E. F. In *High Performance Polymers*; Baer, E., Moet, S., Eds.; Hanser: Munich, 1990; p 79.
(26) Bleha, T.; Gajdos, J.; Karasz, F. E. *Macromolecules* **1990**, *23*, 4076.
(27) Argon, A. S.; Shi, L.-T. *Acta Metall.* **1983**, *31*, 499.
(28) Termonia, Y.; Smith, P. *Macromolecules* **1987**, *20*, 835.
(29) Termonia, Y.; Smith, P. *Macromolecules* **1989**, *21*, 2184.
(30) Termonia, Y.; Smith, P. *Macromolecules* **1988**, *21*, 3485.
(31) Jeffreys, H. *Cartesian Tensors*; Cambridge University Press: Cambridge, UK, 1963.
(32) Mott, P. H.; Argon, A. S.; Suter, U. W. *J. Comput. Phys.* **1992**, *101*, 140.
(33) Van Krevelan, D. W.; Hoftyzer, P. J. *Properties of Polymers—Their Estimation and Correlation with Chemical Structure*; Elsevier: New York, 1976; pp 266, 268, 303.
(34) Yee, A. F., personal communication, 1990.
(35) Wu, W.-L. Ph.D. Thesis, Massachusetts Institute of Technology, 1972.
(36) Brady, T. E.; Yeh, G. S. Y. *J. Appl. Phys.* **1971**, *42*, 12.
(37) Argon, A. S.; Bessonov, M. I. *Philos. Mag.* **1977**, *35*, 917.
(38) Sylvester, M. F.; Yip, S.; Argon, A. S., to be published.

(39) It is to be noted that the commas in the subscripts have been placed for clarity to separate space coordinate information from the atom numbers and do not imply differentiation operations as is customary in tensor algebra. Moreover, it should be noted that in refs 5 and 6 V_i has been used to denote the van der Waals volume of an atom, while in ref 4 it represents the volume of the Voronoi polyhedron of an atom. Here we have used V_i in the latter sense.
(40) As discussed by MAS, the strain increments prescribed by eq 16 will result in small accumulation of second-order reductions in volume. Thus, in practice the actual procedure that was used differed slightly from that given in eq 16 and maintains the volume constant exactly.